ISBN: 978-3-95450-233-2 ISSN: 2673-5504 doi:10.18429/JACoW-SRF2021-TUPFDV010

NEW RECIPES TO OPTIMIZE THE NIOBIUM OXIDE SURFACE FROM FIRST-PRINCIPLES CALCULATIONS*

N. S. Sitaraman†, T. A. Arias, Z. Baraissov, M. M. Kelley, D. A. Muller, M. U. Liepe, R. D. Porter, Z. Sun, Cornell University Department of Physics, 14850 Ithaca, NY

Abstract

The properties of niobium oxide are of critical importance for a wide range of topics, from the behavior of nitrogen during infusion treatments, to the nucleation of Nb_3Sn, to the superconducting properties of the surface. However, the modeling of the oxide is often much simplified, ignoring the variety of niobium oxide phases and the extremely different properties of these phases in the presence of impurities and defects. We use density functional theory (DFT) to investigate how electrochemical treatments and gas infusion procedures change the properties of niobium oxide, and to investigate how these properties could be optimized for Nb_3Sn nucleation and for niobium SRF performance.

INTRODUCTION

The niobium oxide system, which in general may include nitrogen, hydrogen, and other species, is extraordinarily complex, both in the sheer number of phases which may exist and in the wide variety of properties these phases can have. Therefore it is no surprise that modern cavity recipes which alter the oxide surface have been fertile ground for record-breaking niobium and Nb_3Sn SRF cavities, in particular 120C nitrogen-infused niobium cavities and Nb_3Sn cavities grown on pre-anodized niobium [1, 2]. However, we still lack a fundamental understanding of how different chemical conditions affect the composition of the surface oxide, and of how these changes result in improved SRF properties, or improved Nb_3Sn nucleation. If merely scratching the surface, so to speak, of surfaces-by-design has yielded such impressive advances in cavity performance, it behooves us to investigate the oxide surface in detail. Here we present density functional theory (DFT) calculations on niobium oxide; taken together with experimental measurements, they bring us closer to an understanding of the physical mechanisms at hand and potential avenues toward further improvement [3–6].

METHODOLOGY

All calculations are performed within a density-functional theory plane-wave pseudopotential framework using the open-source plane wave software JDFTx [7, 8]. To treat electron exchange and correlation, we use the Perdew-Burke-Ernzerhof (PBE) version of the generalized gradient approximation [9] to the exact density functional. To represent the effects of the atomic cores we employ ultrasoft pseudopotentials [10]. Solvated-surface calculations use the CANDLE polarizable continuum model [11]. To balance charge when calculating energy differences involving the removal of an OH- ion, the initial and final surface state are calculated with excess charge -0.5 and +0.5 respectively. Tc calculations use Eliashberg theory [12] for strong-coupled superconductors within a DFT framework, calculating electron-phonon matrix elements and employing Wannier function methods to integrate smoothly over all scattering processes on a dense momentum-space grid in order to precisely determine phonon linewidths [13, 14]. These linewidths are themselves smoothly interpolated in reciprocal space and integrated to calculate the phonon spectral function, which we then use to estimate T_c using the McMillan formula [15].

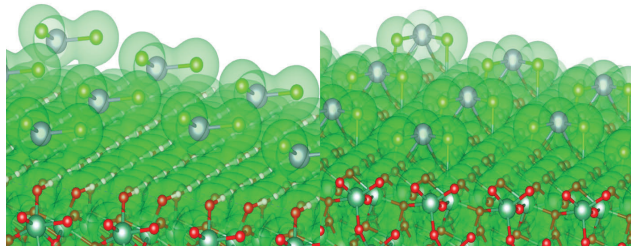

Figure 1: $SnCl_2$ molecules on a Nb_2O_5 surface with (left) and without (right) passivating OH groups covering the surface. An electron density contour is plotted in green.

NUCLEATION OF NB_3SN

Experiments have consistently shown that anodization of the niobium surface produces a thick oxide layer, and that nucleation of Nb_3Sn on this thick oxide results in much more uniform films and higher-performing cavities compared to nucleation on the thin, native niobium oxide surface [16]. Very recently, further experiments have shown that additional modifications to the nucleation step can further improve film uniformity, to the point that it has a shiny appearance as opposed to the usual matte, and a significantly higher quench field than previous Nb_3Sn cavities [2].

It is straightforward to show that the bulk reaction between the Nb_2O_5 oxide and the $SnCl_2$ nucleation agent is not energetically favorable. This immediately makes clear that a more nuanced picture, accounting for surface effects and defects in Nb_2O_5, is necessary in order to adequately describe the nucleation process. Fortunately, an extraordinary amount of research has been done on the low-temperature amorphous phase of Nb_2O_5 with the goal of characterizing its catalytic properties [17]. Our work builds on this research to understand how $SnCl_2$ interacts with a realistic niobium oxide surface.

* Work supported by the U.S. National Science Foundation under Award PHY-1549132, the Center for Bright Beams
† nss87@cornell.edu

ISBN: 978-3-95450-233-2 ISSN: 2673-5504 doi:10.18429/JACoW-SRF2021-TUPFDV010

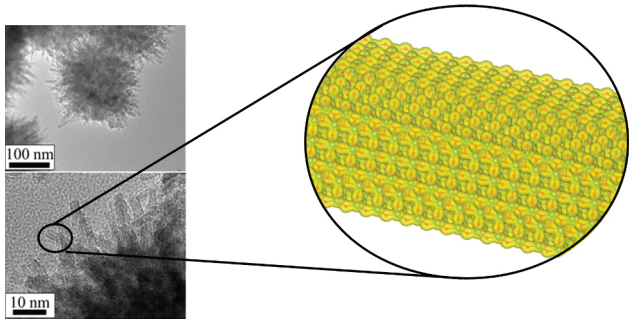

Figure 2: TEM Nb_2O_5 nanoparticle images by Fuchigami, T., and Kakimoto, Ki. (left) compared to our model nanoparticle (right) with electron density shaded in yellow. [18]

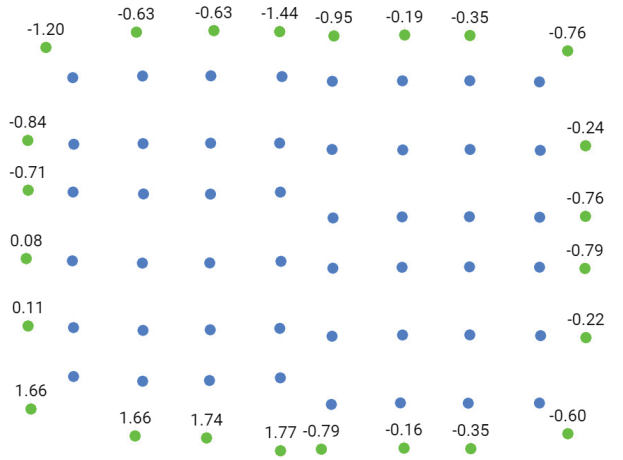

Figure 3: Cross section of Nb_2O_5 nanoparticle, with niobium atoms in blue, and surface binding locations for Cl atoms in green. Binding energies, in eV, are relative to the calculated formation energy per Cl atom of the $SnCl_2$ molecule.

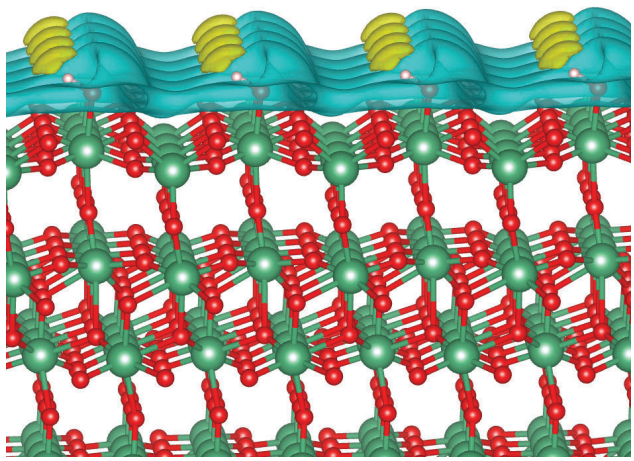

Figure 4: Nb_2O_5 surface for which one of two OH groups per unit cell has been removed. Contours reflect the bound charge density calculated by the polarizable continuum model.

Nb_2O_5 grown under aqueous conditions generally contains some amount of chemisorped H_2O; on the surface this takes the form of OH groups bound to niobium ions. More reduced niobium ions, which lack bound OH groups, are thought to be important sites for catalysis. We find that, as one might expect, the Cl atoms of a $SnCl_2$ molecule bind strongly to these sites, while in the absence of such sites their interaction with the surface is noticeably weaker: Fig. 1. Energetically, the difference between these scenarios is significant when compared to the cohesive energy of $SnCl_2$; the binding energy of $SnCl_2$ to the "active" surface with exposed niobium ions is 0.2 eV stronger than the cohesive energy of $SnCl_2$, while the binding energy to the "passive" surface covered with OH groups is 0.6 eV weaker. At least for this particular surface, it is thermodynamically favorable for $SnCl_2$ to cover the surface only in places with exposed niobium atoms.

In order to gain a deeper understanding of what oxide characteristics are favorable for nucleation, we construct a realistic oxide nanoparticle based on high-resolution SEM images of nanoparticles from [18] (Fig. 2). The nanoparticle has an average surface energy of $0.6\frac{J}{m^2}$, only slightly higher than has been calculated for a perfect Nb_2O_5 surface in the literature ($0.52\frac{J}{m^2}$) [19]. We then investigate how Cl binding energies vary over the surface of the nanoparticle (Fig. 3), and we reach the following conclusions. Firstly, consistent with our calculations on $SnCl_2$ molecules, sites without exposed niobium ions (lower left of cross section) are very unfavorable. Secondly, slight local variations in oxide composition are sufficient to induce changes in binding energy, with locally niobium-rich (oxygen-poor) regions more favorable for binding (e.g. top center). Finally, corner sites are favored over sites on the facets of the crystal.

We now turn our attention to the problem of creating ideal nucleation conditions for Nb_3Sn. In an aqueous environment, OH groups on the surface are in equilibrium with OH- ions in solution, and therefore their equilibrium population on the surface depends on the pH of the solution. For one low-energy Nb_2O_5 surface with two surface niobium ions per unit cell, our calculated binding energies correspond to a critical pH of about 10, below which the first OH group is removed, and 5.5, below which the second OH group is removed (Fig. 4). In general it is likely that binding energies span a much wider range, but we consider this strong evidence that the typical range overlaps with the range of pH readily achievable in experiment. We conclude, therefore, that a low-pH treatment after anodization may result in a significantly higher surface concentration of exposed niobium ions, and better nucleation.

Lastly, we note that the composition of amorphous Nb_2O_5 is known to be highly sensitive to temperature, especially in the range from room temperature to 500C [17]. A first-principles investigation of this temperature dependence is beyond the scope of this work, but it has been observed that increasing temperature is correlated with decreasing surface area, and attenuated catalytic properties, especially beyond about 400C. This is consistent with the latest cavity results,

ISBN: 978-3-95450-233-2 ISSN: 2673-5504 doi:10.18429/JACoW-SRF2021-TUPFDV010

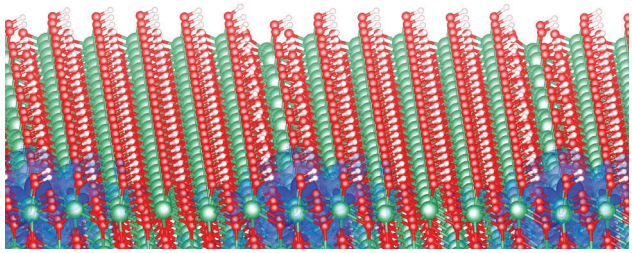

Figure 5: Image of the Nb_2O_5 film surface used for paramagnetic impurity calculations. Blue contours describe the calculated net spin density, which is localized around the site of a missing OH group.

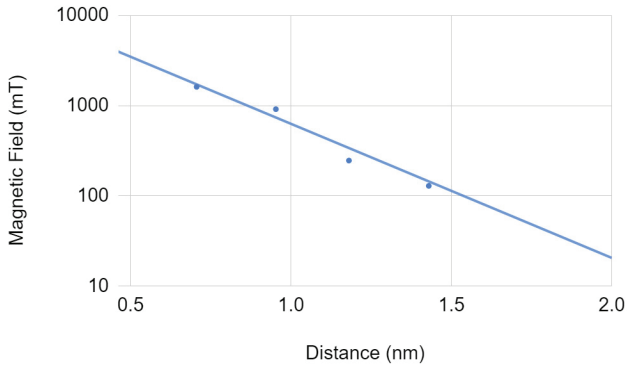

Figure 6: Calculated magnetic field of a paramagnetic impurity in Nb_2O_5 as a function of distance.

which show greatly improved layer uniformity when the $SnCl_2$ nucleation agent is delivered earlier and more rapidly, well before the cavity surface reaches the typical nucleation temperature of 500C [2].

EFFECT OF NB_2O_5 ON SURFACE SUPERCONDUCTIVITY

While Nb_2O_5 is typically considered to be inert in models of the superconducting surface, some researchers have suggested that it may host paramagnetic impurities [20]. Our calculations on defected Nb_2O_5 support this hypothesis, though it is not a simple matter to quantify the effect of such impurities on the surface resistance. Specifically, we find that a simple model treating niobium as a +5 ion, O as a -2 ion, and OH as a -1 ion, can reliably predict the presence of excess electrons in systems where the niobium ions are not fully oxidized. When the concentration of excess electrons is much less than one per niobium ion, i.e. the case of near-stoichiometric Nb_2O_5, these excess electrons are well-described as localized unpaired electrons, each of which exerts a magnetic field on the surrounding material.

To investigate these electrons, we use a thin film of Nb_2O_5 as a model system; each surface niobium ion has an attached OH group, rendering the film perfectly insulating in its undefected state. The removal of any one OH group results in an excess electron localized on the corresponding niobium atom (Fig. 5). We estimate the magnetic field of unpaired electrons in this system by calculating interaction energies for two unpaired electrons at different separations, i.e. by calculating the energy difference between the case where there spins are aligned or opposed, and using the fundamental relation $E = \mu \cdot B$. We find that the field drops off approximately exponentially with distance. As the field is comparable to the RF field at distances of 1-2nm from the unpaired electron, it seems plausible that they have an important effect on the superconducting surface (Fig. 6).

With this understanding, it may be beneficial to minimize the density of unpaired electrons in the native oxide. Evidence in the literature suggests that oxidation in a dry atmosphere proceeds more slowly, possibly reducing the density of defects and their associated unpaired electrons. We observe that unpaired electrons may be eliminated by the addition of OH groups (which accept one electron) or by the replacement of O by N (resulting in the net removal of one electron). While it is easy to verify this in theory, it remains to show what conditions might achieve such defect elimination in practice. Furthermore, it is necessary to extend this research to address the possible magnetic activity of defects and impurities in NbO and niobium.

EFFECT OF NBO+N ON SURFACE SUPERCONDUCTIVITY

NbO is only weakly superconducting, with a Tc of about 1.2K, but NbN with the same rocksalt crystal structure is an excellent superconductor with Tc around 15K. We perform Tc calculations, using DFT and Eliashberg theory, and we find that many intermediate Nb-O-N rocksalt structures are also good superconductors. Based on our calculations both electronic structure and the phonon dispersion play key roles in determining the Tc of a given Nb-O-N rocksalt crystal. Taken together, the low-frequency phonon density of states and the Fermi-level electron density of states can reliably distinguish low-Tc structures (with Tc around 2K) from high-Tc structures (with Tc comparable to or greater than the 9K value for niobium) (Fig. 7).

Given these results, it is tempting to believe that low-T nitrogen infusion recipes could have a beneficial effect on the superconducting properties of the surface by changing the composition of the rocksalt oxide layer, thus increasing the barrier to flux vortex penetration and increasing the superheating field. On the other hand, for such a thin layer, interfacial effects such as epitaxial strain may be highly significant, so it is not clear that system can be approximated as a layer of bulk rocksalt superconductor on top of bulk niobium. We have begun calculations on the phonon dispersion and the Fermi-level electronic density of states in realistic niobium surfaces in order to investigate further.

Our surface phonon calculations, seen in Fig. 8, so far include a bare niobium 100 surface and the NbO ladder structure surface observed experimentally under highly controlled conditions [21]. Both calculations show a very low-frequency peak in the phonon density of states, a characteristic that is correlated with enhanced electron-phonon

ISBN: 978-3-95450-233-2 ISSN: 2673-5504 doi:10.18429/JACoW-SRF2021-TUPFDV010

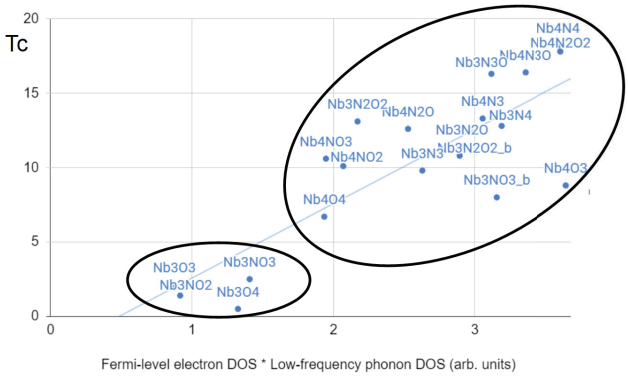

Figure 7: Calculated Tc for rocksalt structures of different compositions, some of which include vacancies. The horizontal axis is the density of phonon states below 16 meV multiplied by the Fermi-level electron density of states, a quantity we find to be correlated with Tc in this system.

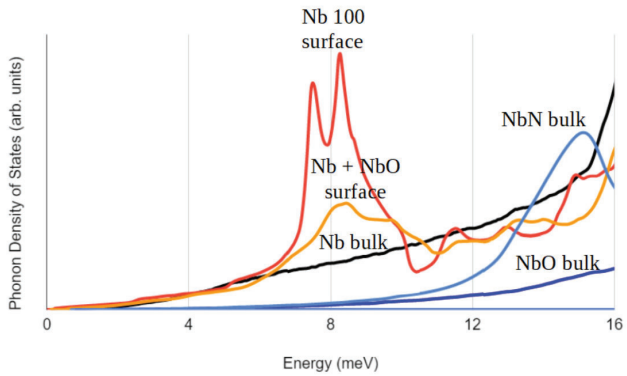

Figure 8: Low-frequency phonon density of states for niobium, NbO, NbN, a niobium surface slab, and a "ladder structure" niobium+NbO surface slab [21]. The density of states peak near 15meV for NbN is responsible in part for its excellent superconducting properties, and we calculate even lower-energy peaks for surface slabs.

coupling in the rocksalt system. Our surface electronic structure calculations are the first, to our knowledge, to explore a realistic native oxide surface from first principles. As expected, Fig. 9 shows a significant dropoff from the high Fermi-level density of states of the underlying bcc niobium to the lower value of NbO (which we note is very similar to the bulk value, despite a strain of several percent necessary to achieve a lattice match with the niobium substrate). Initial attempts at introducing impurities to this system appear have roughly the expected effect, with nitrogen generally enhancing the Fermi-level density of states and hydrogen suppressing it. The effect is non-trivial, especially for the case of nitrogen impurities which actually have the most significant effects away from the nitrogen-doped region.

These preliminary results appear promising for a theory of enhanced (and composition-dependent) surface superconductivity, but more research is needed on different crystal orientations and impurity configurations in order to reach conclusions for a general niobium surface. In addition, we

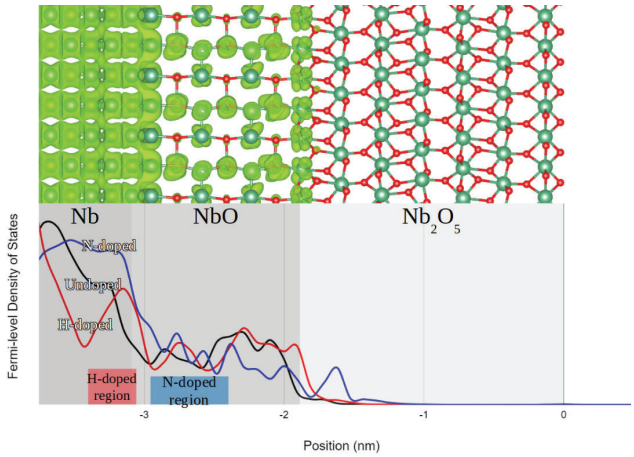

Figure 9: Top: Electronic density of states at the Fermi level vs. position in a native oxide slab calculation. Bottom: Electronic density of states at the Fermi level vs. depth in this calculation (black), and for the same structure with nitrogen (blue) or hydrogen (red) impurities.

emphasize that the relationship between local superconducting properties as a function of depth and the critical field for flux vortex penetration is not yet understood, so it is not yet possible to draw quantitative conclusions about what performance gains we should expect from a given compositional change to the surface.

Finally, we consider the effects of nitrogen on diffusion through the rocksalt oxide layer, a topic of interest as there is mounting experimental evidence that the presence of nitrogen can affect concentrations of other impurities [5]. In its bulk form, the NbO crystal has robustly-ordered vacancies occupying 25% of both niobium and oxygen rocksalt sites; the result is that any oxygen hopping process results in neighboring oxygen and niobium vacancies, an extremely unfavorable configuration described by the large value of over 3 eV at reaction coordinate 0.5 in Fig. 10. Rocksalt niobium nitride, in contrast, generally has much lower vacancy concentrations, and therefore hopping processes do not generally result in neighboring vacancies. A diffusion barrier calculation on a Nb-O-N crystal without niobium vacancies confirms that vacancies on the O-N sublattice lattice diffuse more easily in this case, with a hopping barrier similar to hopping barriers for interstitial impurities in bcc niobium.

The dependence of niobium vacancy concentration on strain and relative oxygen/nitrogen concentration in the rocksalt system has not been studied in detail experimentally, but is likely to be of critical importance for estimating diffusion constants in this system. Our preliminary energetic calculations, which study only the 8-atom rocksalt unit cell, suggest that niobium vacancies become energetically unfavorable (i.e. it is favorable for bcc niobium atoms to fill them) when the nitrogen concentration is equal to or greater than the oxygen concentration. In the near future we plan to collaborate with materials scientists to investigate the ternary Nb-N-O phase diagram in greater detail.

ISBN: 978-3-95450-233-2 ISSN: 2673-5504 doi:10.18429/JACoW-SRF2021-TUPFDV010

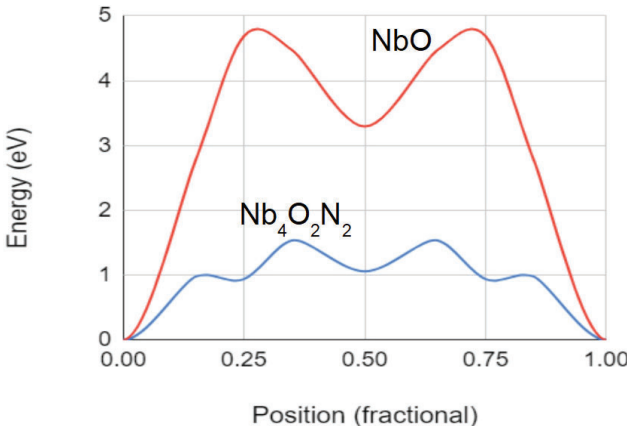

Figure 10: Energy vs. position along the diffusion pathway for the (intrinsic) oxygen-sublattice vacancy in NbO (red) and for a vacancy in rocksalt $Nb_4N_2O_2$ (blue). Both calculations are in a 64-site rocksalt supercell.

CONCLUSIONS

Our first-principles calculations yield new insights into the fundamental physics behind improved Nb_3Sn growth recipes and niobium nitrogen infusion recipes. Specifically, we show that Nb_2O_5 surface properties may be optimized to facilitate the reaction with the $SnCl_2$ nucleation agent, that the concentration of paramagnetic impurities in Nb_2O_5 depends on oxide composition and may affect SRF performance, and that nitrogen incorporation enhances the superconducting and diffusive properties of the rocksalt monoxide layer. These results encourage us to focus on high-pH and low-temperatures processes for Nb_3Sn nucleation, to scrutinize the chemical growth conditions of the native oxide, and to explore (in theory and in practice) a broader range of nitrogen chemical potentials for infusion. Multiple experiments along these lines are already underway, and we anticipate that the results will further advance our understanding of Nb_3Sn growth and the role of oxides on SRF performance.

REFERENCES

[1] A. Grassellino *et al.*, "Unprecedented quality factors at accelerating gradients up to 45 MV/m in niobium superconducting resonators via low temperature nitrogen infusion," *Superconductor Science and Technology*, vol. 30, no. 9, p. 094 004, Aug. 2017.

[2] S. Posen *et al.*, "Advances in Nb_3Sn superconducting radiofrequency cavities towards first practical accelerator applications," *Superconductor Science and Technology*, vol. 34, no. 2, p. 025 007, Jan. 2021.

[3] Z. Sun *et al.*, "Surface oxides onNband Nb_3Sn surfaces: Toward a deeper understanding," presented at SRF'21, Grand Rapids, MI, USA, Jun. 2021, paper THPTEV004, this conference.

[4] E. Lechner, J. Angle, F. Stevie, M. Kelley, C. Reece, and A. Palczewsk, "Sims investigation of furnace baked Nb," presented at SRF'21, Grand Rapids, MI, USA, Jun. 2021, paper THPFDV003, this conference.

[5] S. Chetri, S. Balachandran, P. Dhakal, L. D. Cooley, and P. J. Lee, "Coupon sample characterization of SRF grade high purity Nb treated with high-Q Recipes,"presented at SRF'21, Michigan, USA, Jun. 2021, paper SUPFDV019, this conference.

[6] C. Bate *et al.*, "Nitrogen infusion sample R&D at DESY," presented at SRF'21, Grand Rapids, MI, USA, Jun. 2021, paper SUPFDV001, this conference.

[7] M. C. Payne, M. P. Teter, D. C. Allan, T. A. Arias, and J. D. Joannopoulos, "Iterative minimization techniques for ab initio total-energy calculations: Molecular dynamics and conjugate gradients," *Reviews of Modern Physics*, vol. 64, no. 4, pp. 1045–1097, 1992.

[8] R. Sundararaman, K. Letchworth-Weaver, K. A. Schwarz, D. Gunceler, Y. Ozhabes, and T. A. Arias, "Jdftx: Software for joint density-functional theory," *SoftwareX*, vol. 6, pp. 278–284, Jan. 2017.

[9] J. P. Perdew, K. Burke, and M. Ernzerhof, "Generalized gradient approximation made simple," *Physical Review Letters*, vol. 77, no. 18, pp. 3865–3868, 1996.

[10] K. F. Garrity, J. W. Bennett, K. M. Rabe, and D. Vanderbilt, "Pseudopotentials for high-throughput DFT calculations," *Computational Materials Science*, vol. 81, pp. 446–452, 2014.

[11] R. Sundararaman and W. A. Goddard III, "The charge-asymmetric nonlocally determined local-electric (CANDLE) solvation model," *Journal of Chemical Physics*, vol. 142, no. 6, 2015.

[12] G. M. Eliashberg, "Interactions between electrons and lattice vibrations in a superconductor," *Journal of Experimental and Theoretical Physics (U.S.S.R.)*, vol. 11, no. 3, pp. 966–976, 1960.

[13] N. Marzari and D. Vanderbilt, "Maximally localized generalized Wannier functions for composite energy bands," *Physical Review B - Condensed Matter and Materials Physics*, vol. 56, no. 20, pp. 12 847–12 865, 1997.

[14] A. Habib, F. Florio, and R. Sundararaman, "Hot carrier dynamics in plasmonic transition metal nitrides," *Journal of Optics (United Kingdom)*, vol. 20, no. 6, Jun. 2018.

[15] W. L. McMillan, "Transition temperature of strong-coupled superconductors," *Physical Review*, vol. 167, no. 2, pp. 331–344, 1968.

[16] S. Posen, M. Liepe, and D. L. Hall, "Proof-of-principle demonstration of Nb_3Sn superconducting radiofrequency cavities for high Q_0 applications," *Applied Physics Letters*, vol. 106, no. 8, Feb. 2015.

[17] K. Skrodczky *et al.*, "Niobium pentoxide nanomaterials with distorted structures as efficient acid catalysts," *Nature Communications Chemistry*, vol. 2, no. 129, 2019.

[18] T. Fuchigami and K. Kakimoto, "Spiky niobium oxide nanoparticles through hydrothermal synthesis," *Journal of Materials Research*, vol. 32, pp. 3326–3332, 2017.

[19] M. B. Pinto, A. L. Soares, M. C. Quintão, H. A. Duarte, and H. A. De Abreu, "Unveiling the structural and electronic properties of the b-Nb_2O_5 surfaces and their interaction with H_2O and H_2O_2," *The Journal of Physical Chemistry C*, vol. 122, no. 12, pp. 6618–6628, 2018.

[20] M. Kharitonov, T. Proslier, A. Glatz, and M. J. Pellin, "Surface impedance of superconductors with magnetic impurities," *Phys. Rev. B*, vol. 86, p. 024 514, 2 Jul. 2012.

[21] C. J. Thompson *et al.*, "High temperature persistence and interatomic forces of Nb(100)-(3x1)-O shown by high resolution helium atom scattering and dft calculations," presented at SRF'21, Grand Rapids, MI, USA, Jun. 2021, paper SUPFDV004, this conference.